https://doi.org/10.5194/egusphere-2026-2424
Preprint. Discussion started: 20 May 2026


# The influence of soil moisture on the heavy precipitation event in July 2021 in Western Europe

Till Fohrmann[1], Svenja Szemkus[1], Oliver Heuser[1], Arianna Valmassoi[2], and Petra Friederichs[1]

[1]Institue of Geosciences, University of Bonn, Bonn, Germany
[2]Deutscher Wetterdienst, Data Assimilation and Prediction, Offenbach am Main, Germany

**Correspondence:** Till Fohrmann (tfohrmann@uni-bonn.de)

**Abstract.** Soil moisture-precipitation feedback is an important factor in the water and energy cycles. But how important is it on the time scale of an atmospheric extreme precipitation event? We are investigating this question using the example of heavy precipitation in July 2021, which led to destructive flash floods in Western Europe. To quantify the importance of land-atmosphere coupling and continental moisture sources for the precipitation, we perform numerical simulations with wet, dry and normal soil moisture conditions over Europe. Ensembles of simulations are performed using a global set up of the ICON numerical weather prediction model with a grid refinement over Europe. To account for both the limited predictability and the delayed response of the atmosphere to changes in soil moisture, we use data assimilation to steer the system's development toward the extreme event, but only to the extent necessary so that our interventions in the soil are not undone. We find that the moisture supply of the event crucially depends on continental moisture sources. This result is further confirmed using moisture tracking. Conversely, increased soil moisture only leads to slight precipitation increases, since surface moisture fluxes are energy-limited. Moisture is also important for the development of the near surface low pressure system, which had a central role in the event. Our ensemble simulations also show that there is potential for more devastating events, i.e., more precipitation.

## 1 Introduction

The heavy precipitation over Western Europe in mid July 2021 caused severe flooding, especially in the Ahr, Erft and Meuse river catchments (e.g., Mohr et al., 2022; Ludwig et al., 2023). Generally, such high-impact events require favorable initial conditions, the presence of a large-scale driver, positive (local) feedback and some random component to initiate the evolution (Sillmann et al., 2017). Due to its severity (Group et al., 2021; Lehmkuhl et al., 2022), the July 2021 event has led to a series of studies examining the various factors that contributed to its origin. Many of these studies focus on the influence of anthropogenic factors such as global warming or river management. For example, in a study by Tradowsky et al. (2023), a higher likelihood for this kind of extreme event and an increase in intensity is attributed to climate change. A similar conclusion is given in a rapid attribution assessment of the influence of anthropogenic emissions on the event by Kreienkamp et al. (2021). Using pseudo global warming simulations and a regional climate model, Ludwig et al. (2023) find that precipitation scales according to the Clausius–Clapeyron relationship and find a non-linear effect on flood peaks. This non-linear response to mete-

https://doi.org/10.5194/egusphere-2026-2424
Preprint. Discussion started: 20 May 2026


orological forcing due to local effects is a crucial amplification mechanism in this event. Interactions between meteorological, hydrological and hydromorphological processes are discussed in Mohr et al. (2022). Several studies point to the fact, that the July 2021 flood event in the Ahr Valley could have been worse (Vorogushyn et al., 2025; Thompson et al., 2025; Voit and Heistermann, 2024), either through changes in the large scale dynamics leading to longer persistence, slightly shifted precipitation patterns, or by similarly plausible precipitation events at other times and locations.

The July 2021 event was characterized by a quasi-stationary low pressure system, which came with long-lasting precipitation over the affected region. Because of the circulation pattern, it is plausible that surrounding regions are crucial in supplying moisture, but previous studies have mixed interpretations of which regions are important. Mohr et al. (2022) highlight the importance of sea surface temperature over the North and Baltic Sea, while Tradowsky et al. (2023) report that according to meteorological services, "...warm and very humid air masses [were supplied] to Central Europe from the Mediterranean in a rotating movement." Insua-Costa et al. (2022) and Staal and Koren (2023) discuss the role of North American forests and find that there is no increase in evaporation in Europe prior to the event. Moisture tracking results using WAM2layers (Kalverla et al., 2025) by Weijenborg et al. (2022) indicate that moisture sources were mostly located over the European continent.

Inspired by the latter contribution, we investigate the role of soil moisture as a source of moisture for the July 2021 heavy precipitation event. We conduct global ensemble simulations of the event with the ICON model (Zängl et al., 2015) in accordance to the storyline approach (Shepherd et al., 2018). To this end we perform simulations under different soil moisture scenarios, with a control that uses best-estimate soil moisture conditions, and counterfactual scenarios with prescribed, anomalously dry and wet soil moisture conditions. Since all other conditions remain unchanged, we can attribute changes in the evolution of the precipitation event directly to soil moisture. To distinguish these signals from natural variability, each scenario further includes a set of ensemble simulations with perturbed initial conditions and ICON model parameters.

The ability to predict the behavior of a chaotic system such as the atmosphere is limited (e.g., Charney, 1966; Lorenz, 1996). Consequently, the ability to accurately predict the event deteriorates the further the start of the simulation is away from the onset of the event. This is a problem in our storyline experiment, because it takes time for the moisture that ends up as precipitation during the event to reach the event's location from the point where it entered the atmosphere. The closer the start of the simulation is to the onset of the event, the more moisture has already evaporated, thereby proportionally diminishing the effect of an imposed change in the soil moisture. Therefore, we require a method to constrain the evolution of the system while also interfering with the water cycle as little as possible to not undo changes made to the water cycle via manipulating soil moisture. Because lateral boundary conditions in regional simulation can introduce positive precipitation biases over land (Goergen and Kollet, 2021), we use a global ICON model with a grid refinement over Europe. To constrain the system, we use a limited form of data assimilation (LDA), where data assimilation is applied everywhere except in the region of interest. In this way, the system has greater flexibility to adapt to our modifications in the soil moisture conditions.

We describe the simulation setup and the soil moisture scenarios in Sections 2.1 and 2.2. To track the origin of soil moisture we use WAM2layers of Kalverla et al. (2025) as described in Section 2.3. In Section 3.1, we investigate how the LDA approach affects predictability and discuss how soil moisture impacts the development of the event. Section 3.2 describes the results of

https://doi.org/10.5194/egusphere-2026-2424
Preprint. Discussion started: 20 May 2026


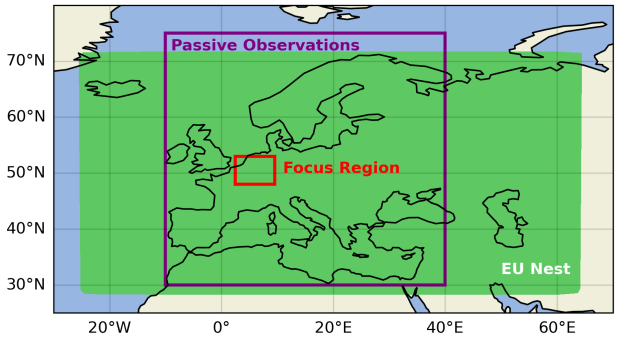


**Figure 1.** Overview of the spatial extents of the EU nest (green), the region in which observations are set to passive in the assimilation scheme (purple) and the focus region (red).

moisture tracking, where according to Weijenborg et al. (2022), we asses the relative importance of source regions. A brief discussion of the main findings can be found in the conclusions Section 4.

## 2 Methods

### 2.1 Simulation Setup

Our atmospheric simulations use the ICON (ICOsahedral Non-hydrostatic) modelling framework (Zängl et al., 2015), which is a development by the German Weather Service (DWD) and the Max Planck Institute for Meteorology (MPI-M). We use ICON in the same configuration as the ICON-DREAM reanalysis (Valmassoi et al., 2025), which in turn is adapted from the operational system at DWD. The simulations are global with a resolution refinement over Europe (EU nest), which is shown in Fig. 1. The refinement follows the common two-way nesting approach with some ICON specific adaptations (Zängl et al., 2015). ICON uses an unstructured triangular grid, which is derived from projecting an icosahedron on a sphere (see Linardakis et al., 2011, for details). Due to this grid construction scheme, the EU nest must have half the grid spacing of the global grid. The grids we use are encoded as R03B07 (R03B08) for the global (EU nest) deterministic run and R02B06 (R02B07) for the global (EU nest) ensemble. The corresponding grid spacings are approximately 13 km (6.5 km) for the global (EU nest) deterministic run and 40 km (20 km) for the global (EU nest) ensemble. Using a global simulation has the advantage that we do not need to prescribe any lateral boundary conditions, as it would be the case with a limited area version of ICON. Since different resolutions require different settings and physical parametrizations, neither global nor nested simulation results are necessarily comparable among themselves. We always analyze results of the global deterministic run at 13 km grid spacing or the EU nest ensemble at 20 km grid spacing, if not stated otherwise.

We perform a set of simulations for each of the three scenarios: A control run with unaltered soil moisture (CTL) as well as a dry and a wet soil moisture scenario denoted as DRY and WET. Details are given in Section 2.2. Each scenario ensemble consists of a deterministic simulation and an ensemble with 20 members at the coarser horizontal resolution. The ensemble

https://doi.org/10.5194/egusphere-2026-2424
Preprint. Discussion started: 20 May 2026


members have perturbed initial conditions as given by the ICON-DREAM ensemble and perturbed physics tuning parameters (see Reinert et al., 2026, for details).

Since the predictability of the event is limited, but the impact of soil moisture onto the atmosphere takes time to fully develop, we constrain the evolution of the atmosphere with data assimilation. Data assimilation in ICON-DREAM follows a hybrid approach consisting of a local ensemble transform Kalman filter combined with a 3D variational method (Reinert et al., 2026). Our assimilation procedure is the same, with the exception that we are limiting the assimilation of observations to everywhere except Europe. All observations over the region marked in Fig. 1 are ignored by setting them to ”passive”, which means they are not assimilated but still available for verification. The passive region is chosen such that the relevant continental moisture source regions - except North America - are included. Otherwise, their contributions would be affected by the observations. Essentially, the assimilation window acts like a soft boundary, because the observation assimilation system draws the atmospheric state towards observations, but does not overwrite it completely. Since the data assimilation is only applied on the global scale, the mismatch between the passive observation region and the EU nest does not affect the result.

Using the limited data assimilation (LDA) enables us to start the simulation on 30 June 2021 at 00 UTC while retaining a sufficiently accurate representation of the event (see Section 3.1) with respect to the precipitation over the focus region (see Fig. 1). The start date was chosen such that there is enough lead time to allow soil moisture to impact the atmosphere in a meaningful way (see Section 3.1). The initial conditions are taken from ICON-DREAM. The simulations end on 15 July 2021 at 21 UTC at which point the peak in precipitation intensity over the focus region has passed.

### 2.2 Soil Moisture Scenarios

We use the default land surface scheme available for ICON called TERRA-ML. The surface model manages the exchange of energy and water at the surface and for several subsurface layers. Only vertical fluxes are considered in TERRA-ML, as there is no exchange with neighboring grid cells. To assess the maximal possible impact of soil moisture on precipitation in our scenarios, we follow the method in Roque Mamani and Valmassoi (2025) and override the update step of soil moisture in TERRA-ML itself. In the CTL simulation, TERRA-ML is used with default settings, i.e., we use the soil moisture analysis to get the best possible estimate of moisture conditions. In the DRY scenario, soil moisture is set to permanent wilting point, i.e., the level of moisture at which plants are no longer able to draw water from the soil. In the WET scenario, soil moisture is set to saturation. In TERRA-ML, these levels are pre-defined for each soil type. This approach effectively disables the land-atmosphere coupling with regard to the water cycle, since precipitation and evapotranspiration continue to take place, but no longer affect soil moisture.

### 2.3 Moisture Tracking

Modifying evaporation caused by changes in the soil moisture might affect the relative importance, or even the spatial distribution, of the moisture source regions relevant to this event. To assess such effects, we use the Water Accounting Model – 2 layers version 3 (WAM2layers; Kalverla et al., 2025). WAM2layers is an offline, Eulerian atmospheric moisture tracking model. As the name suggests, the vertical extent of the atmosphere is divided into an upper and a lower layer. The model then calculates

https://doi.org/10.5194/egusphere-2026-2424
Preprint. Discussion started: 20 May 2026


the amount of water exchanged between grid cells as well as the two vertical layers and keeps track of the moisture, which was "tagged" at the start of the tracking procedure. It is assumed that the horizontal transport of tagged moisture is proportional to the overall moisture transport.

Since we are interested in the moisture sources of the event, the tagged moisture is the precipitation that occurred within the focus region as displayed in Fig. 1 between 13 July 2021 at 00 UTC and 15 July 2021 00 UTC. The tagged moisture is then tracked back to the grid cell where it evaporated, or is considered not tracked if it either leaves the tracking domain or remains in the atmosphere at the end of the tracking process, which is on 1 July 2021 at 00 UTC. We discard the first 24 hours of the simulation to let ICON adapt to the forced soil moisture conditions in the soil moisture scenarios. In our case, the tracking domain reaches from 80° W to 60° E and from 25° N to 65° N. This area was chosen to include the source regions reached within the tracking period.

WAM2layers uses a few simplifications that introduce errors in the tracking results. It only considers specific humidity in the flux calculation, other phases of water are neglected. Also, WAM2layers' budget analysis assumes hydrostatic balance in the vertical integration, which conflicts with ICON's non-hydrostatic dynamical core. Another ICON specific problem is that WAM2layers is currently not pre-configured to work with ICON's triangular grid. We therefore interpolate our hourly simulation output to a geographic coordinate system of 0.15° grid spacing. All of this introduces errors in the tracking results, which we cannot readily correct or quantify, but which apply equally to all simulations.

## 3 Results

### 3.1 Simulation

As discussed above, when choosing the start date of the simulations, there is a conflict of objectives between accurately reproducing the event and allowing for the time required for soil moisture modifications to take effect. To demonstrate this, we use free forecasts with ICON initialized from ICON-DREAM on different dates. Here, we are using the same ensemble setup as described in Section 2.1, but without any data assimilation. Figure 2 demonstrates how the predictability of the event is limited to a couple of days without data assimilation.

To enable a comparison between the simulations, the "event" is defined as the precipitation total between 13 July 2021 00 UTC and 15 July 2021 00 UTC, aggregated over the focus region shown in Fig. 1. We use the ICON-DREAM reanalysis as reference. Of course, the actual precipitation distribution and amounts are associated with large uncertainties (e.g., Kracheletz et al., 2025), but since ICON-DREAM uses the same model and the full set of observations, it is the best point of reference. Since some deviation from the reference in timing and location is permissible, we relax the event definition in the free forecasts. Instead of the aggregated precipitation over a predefined time interval and area, we search for the maximum we can get over a spatio-temporal aggregation window of the same size, if we allow it to be offset by up to 12 h temporally or 3° spatially.

As expected, the amount of precipitation in the free simulations increases the closer the initialization date gets to the start of the event and converges towards the reference, which is the ICON-DREAM reanalysis. We see no evolution into a heavy precipitation event for lead times of 6 days or more. Precipitation totals begin to approach the reference value only at 5 days

https://doi.org/10.5194/egusphere-2026-2424
Preprint. Discussion started: 20 May 2026


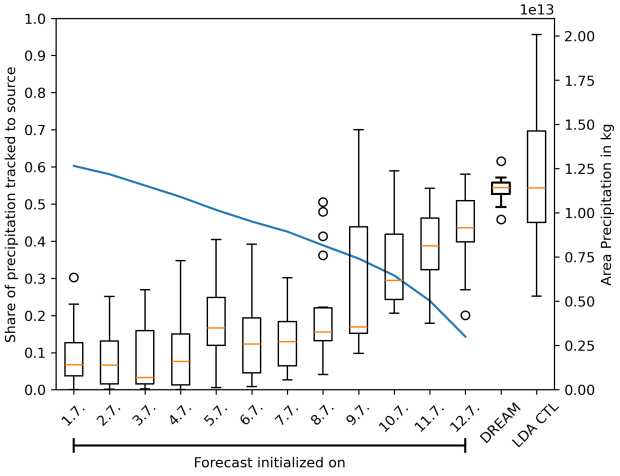


**Figure 2.** Percentage of precipitation in ICON-DREAM (blue line, left axis) that has been tracked back by WAM2layers to it's source up to the given days. The box-whiskers (right axis) indicate the precipitation amounts for "the event" in different simulations, based on the respective 20 member ensembles for the free forecasts with 12 different initial dates at 00 UTC, ICON-DREAM, and CTL (with LDA). For ICON-DREAM and the CTL simulation, precipitation is accumulated over the focus region shown in Fig. 1 between 13 July 2021 00 UTC and 15 July 2021 00 UTC. For the free simulations maximum precipitation amount is shown for the same area and time frame but shifted by up to 12 h temporally or 3° spatially.

and less before the event. The share of precipitation that could be tracked back to it's source region, however, increases with lead time (blue line in Fig. 2), and ranges from about 15 % for a lead time 1 day to 60 % for a lead time of 12 days. For a lead time of 4 days, only 40 % of the precipitation is tracked back, and could potentially be affected by soil moisture, since it has not been evaporated yet. The conclusion is that the time it takes for our changes to soil moisture to fully affect the atmosphere is longer than the prediction horizon in the free forecasts.

Figure 2 also shows the result using the LDA approach in the CTL run. The forecast accuracy in terms of precipitation total is greatly increased, as the ensemble median now corresponds to that of ICON-DREAM. The ensemble spread in the LDA ensemble is much larger, because differences between the ensemble members grow over the 13 day long simulation – at least within the passive observation region (see Fig. 1). It is noteworthy that the ensemble includes simulations showing up to 60 % more precipitation compared to the narrow distribution of the reanalysis, which is in line with other studies that identify potential for an even more severe July 2021 precipitation event (Vorogushyn et al., 2025; Thompson et al., 2025; Voit and Heistermann, 2024).

Maps of simulated precipitation in the deterministic runs are shown in Fig. 3. Shown are 48 h precipitation totals between 13 July 2021 at 00 UTC and 15 July 2021 00 UTC. The general shapes and locations of the precipitation patterns are fairly similar across all simulations. This proves that the LDA approach adequately constrains the large-scale evolution of the system. The CTL simulation (Fig. 3d) produces similar amounts of precipitation as ICON-DREAM (Fig. 3a), although the spatial patterns

https://doi.org/10.5194/egusphere-2026-2424
Preprint. Discussion started: 20 May 2026


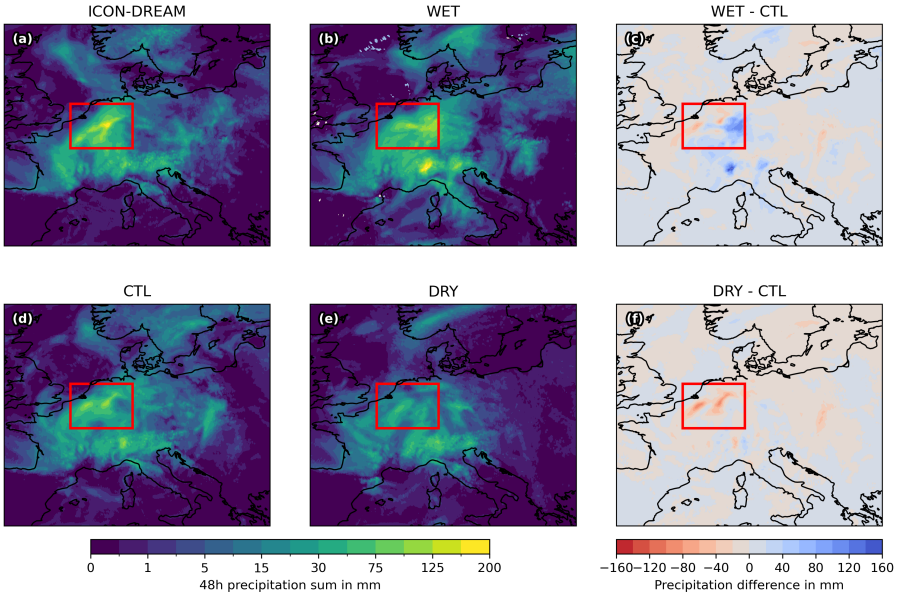


**Figure 3.** Comparison of precipitation totals between 13 July 2021 at 00 UTC and 15 July 2021 00 UTC in the deterministic simulations of (a) ICON-DREAM, (b) the WET, (d) CTL, and (e) DRY scenario. Subfigures (c) and (f) show the differences of the scenarios to the CTL. The red boxes indicate the focus region.

are smoother in the focus region. In the WET scenario (Fig. 3b), the added moisture increases the precipitation amounts substantially compared to the CTL simulation (Fig. 3c) with up to 115 mm less precipitation in parts of the focus region. We also see an eastwards shift of the precipitation hot spot in the WET scenario. The biggest differences appear in the DRY scenario (Fig. 3e), where, compared to the CTL simulation, up to 95 mm less precipitation is generated over 48 h in large parts of the focus region.

While Fig. 3 demonstrates the potential impact of soil moisture on precipitation, it is only one realization of a system with considerable uncertainties. To confirm that the signals are not due to natural variability alone, we present the ensemble information in Fig. 4a as a time series. As with the spatial patterns before, we see a general agreement in the timing of the precipitation over the focus region. All four simulations produce three distinct peaks on the 10th, 13th and 14th of July. Compared to ICON-DREAM, the CTL simulation produces slightly more precipitation of about 5 % over the duration shown in Fig. 4 when comparing the median values. Saturating the soils causes a modest increase in median precipitation of about 10 % compared to the CTL median over the plotted six day time span. Drying the soils has a larger impact of about 36 % less median precipitation compared to CTL.

In the resolutions used here, ICON is not convection permitting, and convective, sub-scale precipitation is generated by the convection parameterization. As can be seen in Fig. 4b, the timeseries of convective precipitation shows that, at least in our simulations, it plays a minor role during the peak of the event. Consequently, changes in soil moisture seem to have little impact on small-scale convective processes in our simulations. We do see, however, a significant impact during the preceding smaller

https://doi.org/10.5194/egusphere-2026-2424
Preprint. Discussion started: 20 May 2026


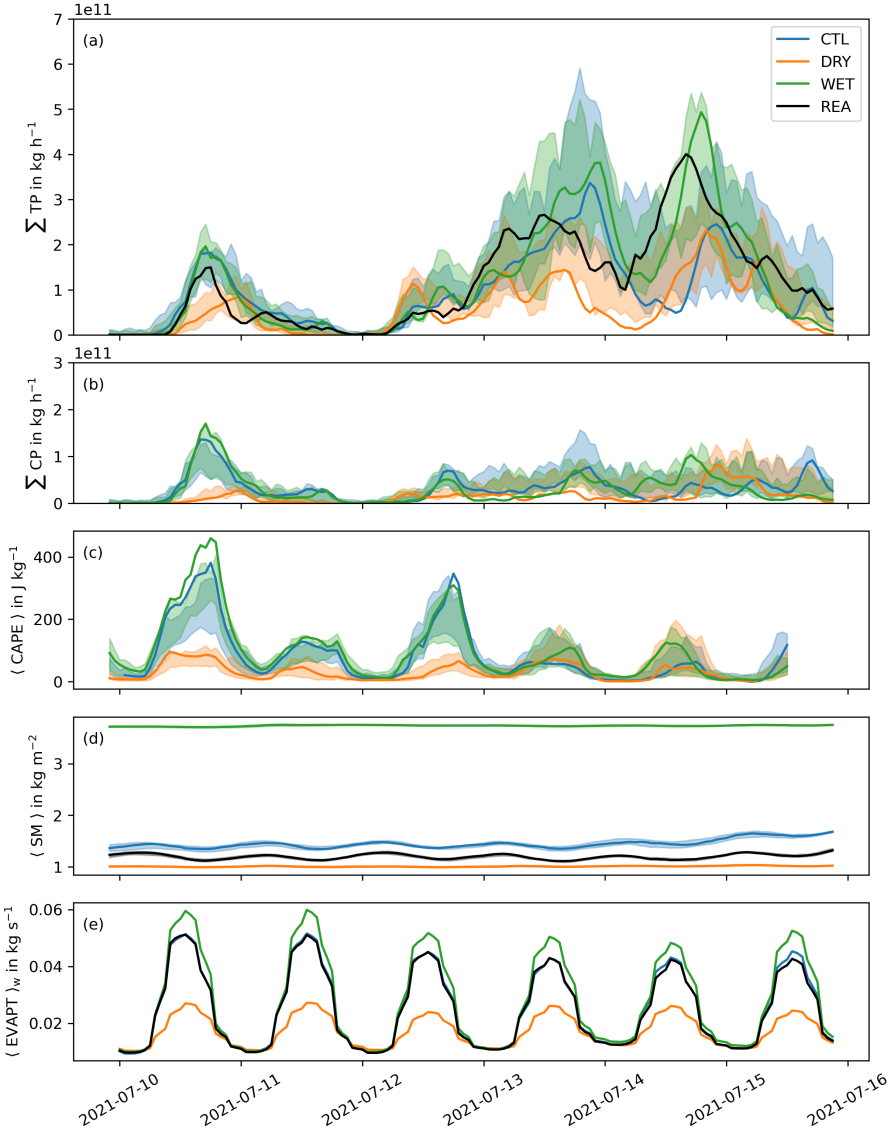


**Figure 4.** Time series of (a) total and (b) convective precipitation hourly rates (de-accumulated) aggregated over the focus region as shown in Fig. 1 in ICON-DREAM (REA), the CTL simulation, the DRY and WET scenario. The solid lines are the deterministic runs, the shaded areas indicate the interquartile ranges of the 20 member ensemble. For ICON-DREAM the interquartile ranges of the ensemble is comparatively small (not shown). (c) CAPE averaged over the focus region. (d) Top level soil moisture averaged over the "Mid-Europe" PRUDENCE region (Christensen and Christensen, 2007). (e) Weighted averages of evapotranspiration rate (instantaneous). The grid cells are weighted according to the amount of evapotranspiration they contributed to the tagged precipitation, as determined by WAM2layers.

precipitation event on 10th July 2021, which evolved due to the formation of a convergence line. Here, the DRY scenario
180 shows a pronounced decrease in precipitation. The lack of moisture in the atmospheric boundary layer also reduces the already

https://doi.org/10.5194/egusphere-2026-2424
Preprint. Discussion started: 20 May 2026


modest values of convective available potential energy (CAPE, Fig. 4c), which further inhibits the formation of small-scale precipitation.

To distinguish changes in precipitation at various spatial scales, we also perform a wavelet analysis according to Szemkus et al. (2025). The results are displayed in Appendix A and confirm our findings from Fig. 4. We observe an increased (decreased) of precipitation amounts in the WET (DRY) scenario relative to the CTL simulation. However, we find no evidence for systematic differences in spatial scales between the scenarios, indicating that the precipitation changes occur consistently across all resolved scales. We further performed a wavelet analysis for temporal scales (not shown), which likewise revealed no systematic differences between the scenarios.

Figure 4d shows the development of top level soil moisture exemplified for the "Mid-Europe" PRUDENCE region (Christensen and Christensen, 2007), which supplies a considerable amount of moisture to the precipitation as will be shown in Section 3.2. The aggregate of top level soil moisture stays fairly constant throughout each experiment. This is expected in the WET and DRY scenarios, since soil moisture is forced to saturation or wilting point. But also the CTL and ICON-DREAM top level soil moisture exhibits only small variations on this short timescale. Even more interesting is the fact that it is the WET scenario, which strongly deviates from the others. During this period, the median of top level soil moisture in the WET scenario is about 161 % higher than that of the control run. In the DRY scenario it is about 30 % less. Considering that the precipitation responds stronger to the dry conditions than the wet conditions demonstrates the non-linear response of precipitation to soil moisture.

From a synoptic point of view, our understanding of the processes that lead to the enhanced (reduced) precipitation in the WET (DRY) scenario is the following: Inspecting the ensemble members, we see that the large-scale synoptic pattern is mostly unaffected by the moisture changes. However, variables and processes within the atmospheric boundary layer undergo substantial modifications, particularly in the DRY scenario. Here, the drastic reduction in evapotranspiration as seen in Fig. 4e most likely leads to an increase in sensible heat flux, while the latent heat flux strongly decreases. A reduced latent heat flux limits evaporative cooling, ultimately resulting in higher near-surface temperatures during daytime. Indeed, average 2 m temperature increases by $1.96 \pm 0.99$ K across the DRY ensemble compared to the CTL run during the event in the focus region. At the same time, the enhanced sensible heat flux likely strengthens buoyancy-driven turbulence, promoting stronger entrainment of dry air into the atmospheric boundary layer.

Due to the limited surface moisture supply and enhanced entrainment, specific humidity is substantially lower and more spatially confined in the DRY scenario compared to the WET and CTL runs. Although warmer air can hold more moisture, the lack of moisture input causes a pronounced decline in the relative humidity and the total column integrated water vapor (TQV). Averaging over the focus region, relative humidity drops by $5 \pm 3$ % in the DRY scenario during the event depending on the ensemble member, but the spatial variability is large. As an example, TQV is shown for 14 July 2021 at 12 UTC in Appendix B. We think that, as a consequence of reduced boundary-layer moisture and increased entrainment of dry free-tropospheric air, the lifting condensation level is likely to rise and parcel buoyancy to decrease, thereby suppressing convective initiation despite higher surface temperatures.

https://doi.org/10.5194/egusphere-2026-2424
Preprint. Discussion started: 20 May 2026


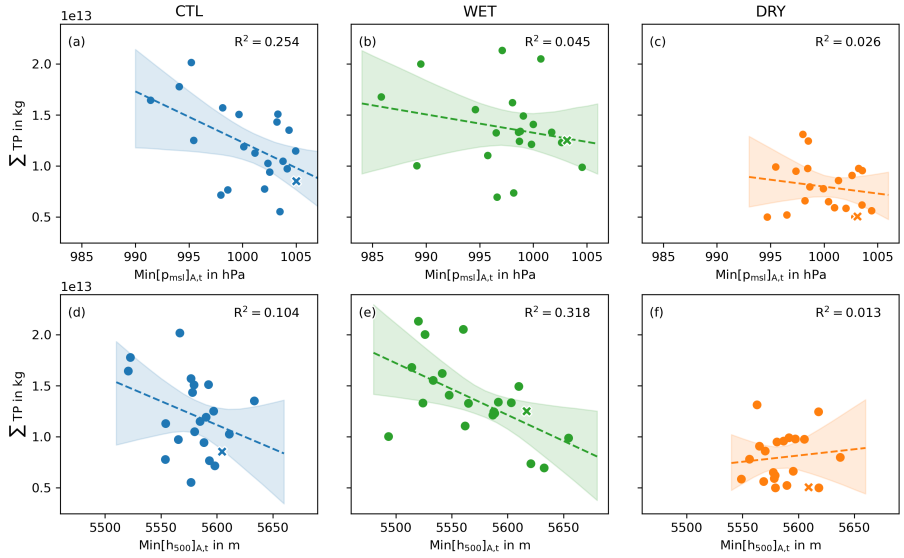


**Figure 5.** Scatter plots of precipitation totals against the minima in (a)-(c) sea level pressure and (d)-(e) 500 hPa geopotential height. Totals are calculated over the focus region as shown in Fig. 1 and between 13 July 2021 at 00 UTC and 15 July 2021 00 UTC. For the minima in sea level pressure and geopotential height, the focus region is expanded by 2° in all directions. The deterministic runs are marked with crosses, the ensemble members with dots. The dashed lines are linear fits to the data with estimated confidence intervals to a level of 95 % indicated by the shaded areas.

An additional notable difference is found in the development of the surface low that played a key role in the Western European flood event. The dynamic circulation patterns of the ensemble members remain largely consistent. The variation within the ensemble is primarily evident in the strength of the dynamic circulation, which is reflected in fluctuations in the core pressure at the surface. We find an associated pronounced spread in core sea level pressure (SLP) across ensemble members. Figure 5a–c shows precipitation sums against the lowest value in SLP found throughout the event in each scenario and ensemble member. The minimum is taken with respect to an area corresponding to the focus region but expanded by 2° in all directions. We find that increased soil moisture enables the formation of stronger lows and vice versa. Figure 5d–f shows a similar relationship for the geopotential trough at the 500 hPa level, which also deepens with increased moisture. Given our synoptic understanding, we attribute the general formation mechanism of the surface low to upper troposphere divergence, on which humidity is likely to only have an indirect effect. However, increased humidity appears to intensify the low-pressure system, most likely through latent heat release. Figure 5 also shows that ensemble members with lower core SLP or a deeper 500 hPa geopotential height trough generally produce more precipitation. Some of the scatter plots in Fig. 5 show a positive linear relationship. The explained variance between the trough depth at 500 hPa and the total precipitation in the WET ensemble amounts to about 31 %. Although these are not the only explanatory variables and the variability is high, the 95 % confidence intervals of the regression lines indicate a positive correlation in CTL for SLP and in WET for the 500 hPa trough depth.

https://doi.org/10.5194/egusphere-2026-2424
Preprint. Discussion started: 20 May 2026


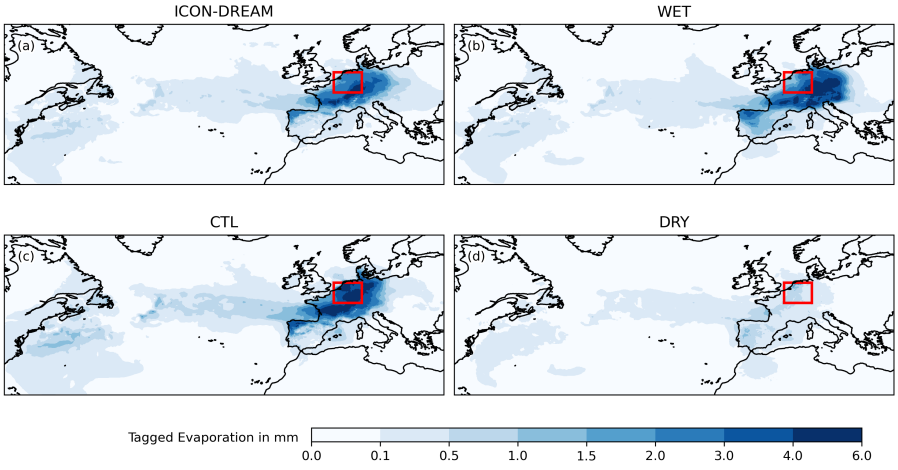


**Figure 6.** Moisture source regions for precipitation between 13 July 2021 at 00 UTC and 15 July 2021 00 UTC over the focus region (see Fig. 1). The back-tracking was performed using WAM2layers (Kalverla et al., 2025). Percentages of tracked moisture are 60,% in ICON-DREAM, 56 % in the CTL simulation, 66 % in WET and 52 % in the DRY scenario.

## 3.2 Moisture Sources

**Table 1.** Amount of moisture backtracked to the given region in each simulation using WAM2layers. For the continental regions, we use the PRUDENCE regions (Christensen and Christensen, 2007), i.e., the British Isles (BI), the Iberian Peninsula (IP), France (Fr), Mid-Europe (ME), Scandinavia (SC), the Alpine region (AL), the Mediterranean region (ME) and East Europe (EA). We also show values for the Mediterranean Sea (MeS), the Baltic Sea (BaS), the North Sea (NoS), the West European shelf (WES) and the North Atlantic (NAt). Values are given as percentages compared to the total amount of tracked moisture.

| Sim. | BI | IP | FR | ME | SC | AL | MD | EA | MeS | BaS | NoS | WES | NAt |
|---|---|---|---|---|---|---|---|---|---|---|---|---|---|
| REA | 0.4 | 6.4 | 11.6 | 22.4 | 0.4 | 8.9 | 0.7 | 5.4 | 2.6 | 0.2 | 0.7 | 4.9 | 30.1 |
| CTL | 0.6 | 7.0 | 11.9 | 21.1 | 0.8 | 7.4 | 0.3 | 1.5 | 2.4 | 0.3 | 0.9 | 5.7 | 34.6 |
| DRY | 0.4 | 11.7 | 5.5 | 7.5 | 0.1 | 2.8 | 0.7 | 0.3 | 5.8 | 0.1 | 1.3 | 6.8 | 45.7 |
| WET | 0.3 | 10.2 | 9.2 | 22.8 | 0.3 | 13.2 | 1.4 | 7.1 | 2.9 | 0.2 | 0.3 | 3.8 | 22.9 |

Tracking experiments were performed for ICON-DREAM and all of our simulations as outlined in Section 2.3. We list shares of tracked moisture for selected regions in Table 1 for a quantitative comparison. Figure 6 gives a qualitative overview of the resulting moisture source regions. Figure 6 shows that the spatial distribution of source regions is fairly similar across the four datasets indicating that the large scale circulation is effectively constrained using the LDA approach. In all cases, the largest contributors are the North Atlantic and Mid-Europe. The differences lie in the relative importance of the source regions. As with precipitation above, it is the DRY scenario, which stands apart. Here, evapotranspiration is severely limited.

https://doi.org/10.5194/egusphere-2026-2424
Preprint. Discussion started: 20 May 2026


Consequently, maritime moisture sources - especially the North Atlantic - contribute considerably more of the overall moisture compared to the other simulations. At the same time, less precipitation in the dry scenario means that less moisture is being tracked, which is why we see less contribution of the North Atlantic in absolute terms in Fig. 6. In the WET scenario, the high soil moisture increases the relative contribution of all continental moisture source regions at the expense of maritime sources. Since the WET scenario only sees a slight increase in precipitation compared to CTL, this also implies an absolute shift, e.g., less tagged evaporation over the North Atlantic under wet conditions compared to CTL, as can be seen in Fig. 6.

In Section 3.1, we already discussed the non-linear response of precipitation to soil moisture. Using the tracking results, we can identify which regions are relevant for the precipitation during the event and use them as a basis for comparison. Figure 4e shows a weighted average of evapotranspiration during each simulation. Weights are assigned to each grid point based on the proportion of moisture that has contributed to the tagged precipitation across all simulations, i.e.,

$$w_p = A_p \frac{\sum_{s,t} e_{s,t,p}}{\sum_{s,t,p} e_{s,t,p}} \tag{1}$$

where $w_p$ is the weight assigned to a specific grid point, $A_p$ it's area, $e$ the evaporation that contributed to the tagged precipitation at a specific grid point and time in a given simulation and the summations are over the simulation $s$, time $t$ and grid point $p$. The evapotranspiration timeseries in Fig. 4e therefore mostly reflect the shaded areas in Fig. 6. We can tell from Fig. 4e that evapotranspiration in the relevant source regions is limited not by the availability of moisture, but by the availability of energy: Even though Fig. 4d demonstrates that actual soil moisture levels are closer to permanent wilting point than to saturation, evapotranspiration increases less sharply with saturated soils than it decreases with dried-out soils. This is a well-known response (e.g., Seneviratne et al., 2010). Since we only consider regions that contribute to the event's precipitation, this relationship also explains why the precipitation signal is stronger in the DRY scenario.

## 4 Conclusions

In this study, we simulated the heavy precipitation event in July 2021 under extreme soil moisture conditions. To achieve sufficient accuracy in the realism of the simulated event, we constrained the large scale evolution of the system by using data assimilation. Limiting data assimilation to everywhere except a European region allowed us to have two weeks of lead-time, which is enough time for the planetary surface to influence the atmosphere in a meaningful way and allows dynamical changes to unfold.

Our results show that the soils of the European continent are a highly relevant source region, and that evapotranspiration is energy-limited, as removing soil moisture produces a disproportionally stronger response in surface moisture flux and ultimately in precipitation. We observe changes in the atmospheric boundary layer that are related to soil moisture, but convective processes only account for a fraction of the total precipitation. Wavelet analysis of the precipitation fields also shows no shifts in spatial and temporal scales. Given that, for example, Lenderink et al. (2025) find that their convection-permitting downscaling simulation shows an increased response to their pseudo-global warming signal, it is possible that a lack of small-scale response is partly attributable to the resolution of our model. Like other studies (Vorogushyn et al., 2025; Thompson et al.,

https://doi.org/10.5194/egusphere-2026-2424
Preprint. Discussion started: 20 May 2026


2025; Voit and Heistermann, 2024), our ensemble shows the potential for more severe events, especially in the wet scenario. At the synoptic scale we see that increased soil moisture favors the intensification of the near surface low pressure system.

We show that continental moisture sources are essential for the development of the July 2021 event, as the rainfall would not have been as heavy under dry conditions. This is confirmed by the results of the moisture tracking. Our results contrast with Mohr et al. (2022) and Tradowsky et al. (2023), as we observe only minor contributions of moisture from the North Sea, the Baltic Sea or the Mediterranean, which would suggest that SST anomalies are not decisive for the development of the event. Since any moisture tracking is subject to inherent methodological uncertainties, it would be ideal to carry out further storyline simulations under various SST scenarios in the future.

*Code and data availability.* The code for generating the presented figures and table is available at https://github.com/tfohrmann/july21_eval. The corresponding data is available at https://doi.org/10.5281/zenodo.19818501.

## Appendix A: Spatial scale analysis using wavelets

We apply a wavelet transform to deterministic model simulations to examine structural changes in spatial precipitation fields. The analysis focuses on the EU nest region (Fig. 1), which is interpolated to geographical coordinates on a regular grid with a spacing of approximately 7 km. We employ the dual-tree complex wavelet transform (Kingsbury, 1998), which is particularly well suited for analyzing spatial precipitation fields due to its approximate shift invariance and improved directional selectivity (see, e.g., Szemkus et al., 2025; Buschow, 2024). The transform decomposes the precipitation field into scale-dependent components, providing a localized spectral representation that enables the quantification of spatial variability as a function of scale. We interpret the resulting wavelet energy as a measure of scale-dependent variance.

To reduce artifacts arising from the finite domain, the precipitation fields are linearly smoothed to zero over the outermost 15 grid points prior to the transformation. A two-dimensional wavelet transform is then applied at each time step, yielding the spectral energy distribution across discrete spatial scales of $(7 \cdot 2^0, 7 \cdot 2^1, \ldots, 7 \cdot 2^8)$ km. This results in a wavelet spectrogram for each time step, describing the temporal evolution of variability across spatial scales.

Figure A1 shows the time series of the wavelet spectrogram for the CTL simulation, while for the WET and DRY simulations, differences relative to the control (WET–CTL and DRY–CTL) are presented. Consistent with Fig. 4, total variance increases (decreases) in the WET (DRY) scenario relative to the control simulation. Notably, these changes occur across all resolved spatial scales.

https://doi.org/10.5194/egusphere-2026-2424
Preprint. Discussion started: 20 May 2026


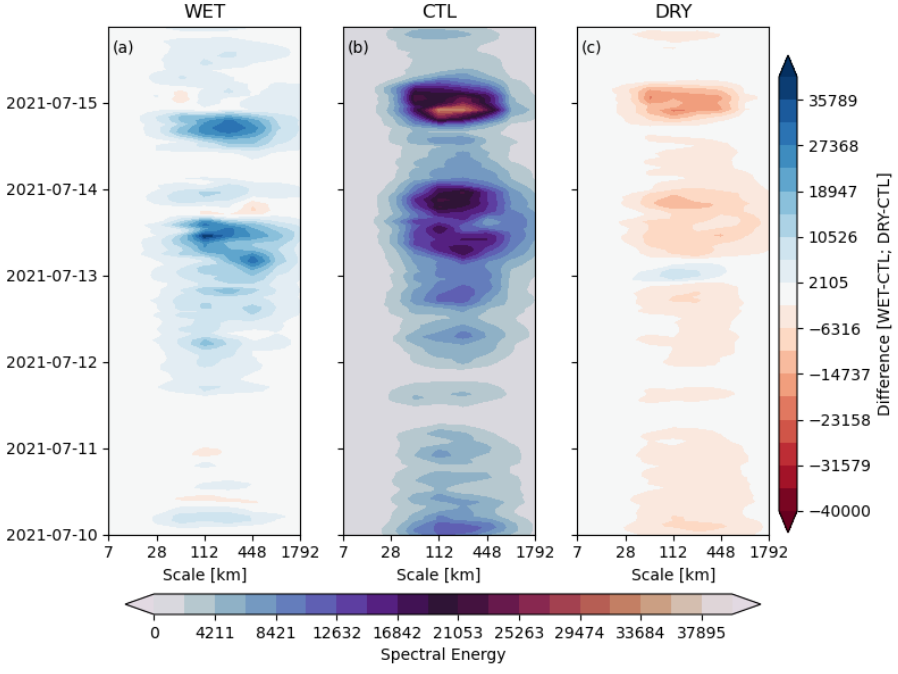


**Figure A1.** Time series of the wavelet spectrogram from deterministic simulations over the EU nest region based on a dual-tree complex wavelet transform. Shown are the control simulation (b) and difference plots for the WET (a; WET–CTL) and DRY (c; DRY–CTL) scenarios.

https://doi.org/10.5194/egusphere-2026-2424
Preprint. Discussion started: 20 May 2026


## Appendix B: Total column integrated water vapor in the scenarios

Figure B1 shows an example of the TQV in the deterministic runs of the scenarios on 14 July 2021 at 12 UTC. A clear decrease in moisture can be seen in the dry soil moisture scenario. At this particular point in time, the decrease is mostly concentrated on Eastern Europe.

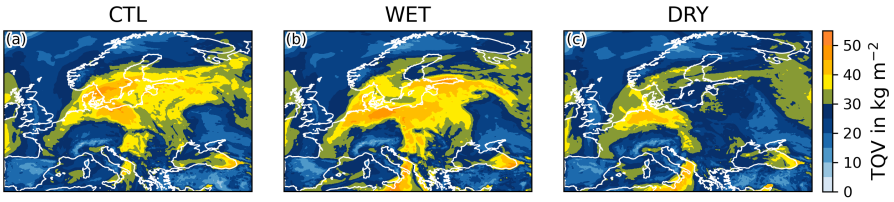


**Figure B1.** Map of total column vapor in (a) the deterministic CTL simulation, (b) the WET and (c) the DRY scenarios. Values are shown for 14 July 2021 at 12 UTC.

*Author contributions.* Conceptualization by TF, AV and PF; methodology by TF and AV; analysis by TF, SS and OH; supervision by AV and PF; writing by TF, SS, OH and PF.

*Competing interests.* There are no competing interests to declare.

*Acknowledgements.* We thank Jane Roque for sharing her method of manipulating soil moisture in TERRA-ML. We thank Imme Benedict and Chris Weijenborg from University of Wageningen for their insights regarding the moisture transport during the event and technical support in using the WAM2layers moisture tracking software. We acknowledge funding by the Deutsche Forschungsgemeinschaft (DFG, German Research Foundation) within the CRC DETECT (SFB 1502/1–2022—Project number 450058266), and the Bundesministerium für Forschung, Technologie und Raumfahrt within the project ClimXtreme II - Module B (BMFTR FKZ 01LP2323A).

https://doi.org/10.5194/egusphere-2026-2424
Preprint. Discussion started: 20 May 2026


## References

Buschow, S.: Tropical convection in ERA5 has partly shifted from parameterized to resolved, Quarterly Journal of the Royal Meteorological Society, 150, 436–446, 2024.

Charney, J. G.: The feasibility of a global observation and analysis experiment, Bull. Amer. Meteor. Soc., 47, 200–230, 1966.

Christensen, J. H. and Christensen, O. B.: A summary of the PRUDENCE model projections of changes in European climate by the end of this century, Climatic change, 81, 7–30, 2007.

Goergen, K. and Kollet, S.: Boundary condition and oceanic impacts on the atmospheric water balance in limited area climate model ensembles, Scientific Reports 2021 11:1, 11, 1–13, https://doi.org/10.1038/s41598-021-85744-y, 2021.

Group, C. F. D. A. F., Schäfer, A., Mühr, B., Daniell, J., Ehret, U., Ehmele, F., Küpfer, K., Brand, J., Wisotzky, C., Skapski, J., Rentz, L., Mohr, S., and Kunz, M.: Hochwasser Mitteleuropa, Juli 2021 (Deutschland) : 21. Juli 2021 – Bericht Nr. 1 "Nordrhein-Westfalen & Rheinland-Pfalz", https://doi.org/10.5445/IR/1000135730, 2021.

Insua-Costa, D., Senande-Rivera, M., Llasat, M. C., and Miguez-Macho, G.: The central role of forests in the 2021 European floods, Environmental Research Letters, 17, 064 053, 2022.

Kalverla, P., Benedict, I., Weijenborg, C., and Van Der Ent, R. J.: Atmospheric moisture tracking with WAM2layers v3, Geoscientific Model Development, 18, 4335–4352, 2025.

Kingsbury, N.: The dual-tree complex wavelet transform: a new efficient tool for image restoration and enhancement, in: 9th European Signal Processing Conference (EUSIPCO 1998), pp. 1–4, IEEE, ISBN 978-960-7620-06-4, 1998.

Kracheletz, M., Liu, Z., Springer, A., Kusche, J., and Friederichs, P.: Would the 2021 Western Europe Flood Event Be Visible in Satellite Gravimetry?, Journal of Geophysical Research: Atmospheres, 130, e2024JD042 190, https://doi.org/10.1029/2024JD042190, _eprint: https://agupubs.onlinelibrary.wiley.com/doi/pdf/10.1029/2024JD042190, 2025.

Kreienkamp, F., Philip, S. Y., Tradowsky, J. S., Kew, S. F., Lorenz, P., Arrighi, J., Belleflamme, A., Bettmann, T., Caluwaerts, S., Chan, S. C., Ciavarella, A., De Cruz, L., de Vries, H., Demuth, N., Ferrone, A., Fischer, r. M., Fowler, H. J., Goergen, K., Heinrich, D., Henrichs, Y., Lenderink, G., Kaspar, F., Nilson, E., Otto, F. E. L., Ragone, F., Seneviratne, S. I., Singh, R. K., Skålevåg, A., Termonia, P., Thalheimer, L., van Aalst, M., Van den Bergh, J., Van de Vyver, H., Vannitsem, S., van Oldenborgh, G. J., Van Schaeybroeck, B., Vautard, R., Vonk, D., and Wanders, N.: Rapid attribution of heavy rainfall events leading to the severe flooding in Western Europe during July 2021, World Weather Atribution, http://hdl.handle.net/1854/LU-8732135, 2021.

Lehmkuhl, F., Schüttrumpf, H., Schwarzbauer, J., Brüll, C., Dietze, M., Letmathe, P., Völker, C., and Hollert, H.: Assessment of the 2021 summer flood in Central Europe, Environmental Sciences Europe, 34, 107, https://doi.org/10.1186/s12302-022-00685-1, 2022.

Lenderink, G., de Vries, H., van Meijgaard, E., de Rooy, W., van Ulft, L., Thompson, V., Qiu, X., and Fowler, H. J.: A pseudo global warming based system to study how climate change affects high impact rainfall events, Weather and Climate Extremes, 49, 100 781, https://doi.org/10.1016/j.wace.2025.100781, 2025.

Linardakis, L., Reinert, D., and Gassmann, A.: Icon grid documentation, Tech. rep., DKRZ Hamburg, https://scivis2017.dkrz.de/hd-cp-2/en-icon_grid.pdf, 2011.

Lorenz, E. N.: Predictability: A problem partly solved, in: Proc. Seminar on predictability, vol. 1, pp. 1–18, Reading, 1996.

Ludwig, P., Ehmele, F., Franca, M. J., Mohr, S., Caldas-Alvarez, A., Daniell, J. E., Ehret, U., Feldmann, H., Hundhausen, M., Knippertz, P., et al.: A multi-disciplinary analysis of the exceptional flood event of July 2021 in central Europe–Part 2: Historical context and relation to climate change, Natural Hazards and Earth System Sciences, 23, 1287–1311, 2023.

https://doi.org/10.5194/egusphere-2026-2424
Preprint. Discussion started: 20 May 2026


Mohr, S., Ehret, U., Kunz, M., Ludwig, P., Caldas-Alvarez, A., Daniell, J. E., Ehmele, F., Feldmann, H., Franca, M. J., Gattke, C., et al.: A multi-disciplinary analysis of the exceptional flood event of July 2021 in central Europe. Part 1: Event description and analysis, Natural Hazards and Earth System Sciences Discussions, 2022, 1–44, 2022.

Reinert, D., Prill, F., Frank, H., Denhard, M., Baldauf, M., Schraff, C., Gebhardt, C., Marsigli, C., Förstner, J., Zängl, G., Schlemmer, L., Blahak, U., and Welzbacher, C.: DWD Database Reference for the Global and Regional ICON and ICON-EPS Forecasting System v2.5.4, https://www.dwd.de/SharedDocs/downloads/DE/modelldokumentationen/nwv/icon/icon_dbbeschr_aktuell.html, 2026.

Roque Mamani, J. L. and Valmassoi, A.: How do Irrigation Schemes shape the Irrigation Impact? A Sensitivity Test with the Operational ICON-NWP, Authorea Preprints, https://doi.org/10.22541/ESSOAR.176530330.04410565/V1, 2025.

Seneviratne, S. I., Corti, T., Davin, E. L., Hirschi, M., Jaeger, E. B., Lehner, I., Orlowsky, B., and Teuling, A. J.: Investigating soil moisture–climate interactions in a changing climate: A review, Earth-Science Reviews, 99, 125–161, 2010.

Shepherd, T. G., Boyd, E., Calel, R. A., Chapman, S. C., Dessai, S., Dima-West, I. M., Fowler, H. J., James, R., Maraun, D., Martius, O., et al.: Storylines: an alternative approach to representing uncertainty in physical aspects of climate change, Climatic change, 151, 555–571, 2018.

Sillmann, J., Thorarinsdottir, T., Keenlyside, N., Schaller, N., Alexander, L. V., Hegerl, G., Seneviratne, S. I., Vautard, R., Zhang, X., and Zwiers, F. W.: Understanding, modeling and predicting weather and climate extremes: Challenges and opportunities, Weather and climate extremes, 18, 65–74, 2017.

Staal, A. and Koren, G.: Comment on 'The central role of forests in the 2021 European floods', Environmental Research Letters, 18, 048 002, 2023.

Szemkus, S., Buschow, S., and Friederichs, P.: Revealing the structure of precipitation extremes: a spatio-temporal wavelet approach, EGUsphere, pp. 1–22, https://doi.org/10.5194/egusphere-2025-5922, publisher: Copernicus GmbH, 2025.

Thompson, V., Coumou, D., Beyerle, U., Ommer, J., Cloke, H. L., and Fischer, E.: Alternative rainfall storylines for the Western European July 2021 floods from ensemble boosting, Communications Earth & Environment, 6, 427, https://doi.org/10.1038/s43247-025-02386-y, publisher: Nature Publishing Group, 2025.

Tradowsky, J. S., Philip, S. Y., Kreienkamp, F., Kew, S. F., Lorenz, P., Arrighi, J., Bettmann, T., Caluwaerts, S., Chan, S. C., De Cruz, L., et al.: Attribution of the heavy rainfall events leading to severe flooding in Western Europe during July 2021, Climatic Change, 176, 90, 2023.

Valmassoi, A., Anlauf, H., Becker, A., Keller, J. D., Krebber, S., Zängl, G., Potthast, R., Cress, A., Fundel, F., Hanisch, T., Lange, M., Steinert, T., and Kaspar, F.: ICON-DREAM: ICON-Dual resolution Reanalysis for Emulators, Applications and Monitoring The ICON-Dual resolution reanalysis version v1.0, https://doi.org/10.5676/dwd/icon-dream_v1, 2025.

Voit, P. and Heistermann, M.: A downward-counterfactual analysis of flash floods in Germany, Natural Hazards and Earth System Sciences, 24, 2147–2164, https://doi.org/10.5194/nhess-24-2147-2024, publisher: Copernicus GmbH, 2024.

Vorogushyn, S., Han, L., Apel, H., Nguyen, V. D., Guse, B., Guan, X., Rakovec, O., Najafi, H., Samaniego, L., and Merz, B.: It could have been much worse: spatial counterfactuals of the July 2021 flood in the Ahr Valley, Germany, Natural Hazards and Earth System Sciences, 25, 2007–2029, https://doi.org/10.5194/nhess-25-2007-2025, publisher: Copernicus GmbH, 2025.

Weijenborg, C., Benedict, I., Polak, F., Vermeulen, T., Kalverla, P., and Sodemann, H.: Moisture origin of the extreme precipitation event in Western Europe in July 2021, https://doi.org/https://doi.org/10.5194/ems2022-407, 2022.

https://doi.org/10.5194/egusphere-2026-2424
Preprint. Discussion started: 20 May 2026


380 Zängl, G., Reinert, D., Rípodas, P., and Baldauf, M.: The ICON (ICOsahedral Non-hydrostatic) modelling framework of DWD and MPI-M: Description of the non-hydrostatic dynamical core, Quarterly Journal of the Royal Meteorological Society, 141, 563–579, https://doi.org/10.1002/QJ.2378, 2015.